 http://dx.doi.org/10.14500/aro.10949

A Computational Model for Temperature Monitoring During Human Liver Treatment by Nd: YaG Laser Interstitial Thermal Therapy (LITT)

Bazhdar N. Mohammed and Dilshad S. Ismael

Department of Physics, College of Science, Salahaddin University-Erbil,
Erbil 44001, Kurdistan Region - F.R. Iraq

***Abstract*—Describing heat transfer in biological organs is absolutely challenging because it is involved with many complex phenomena. Therefore, understanding the optical and thermal properties of living system during external irradiation sources such as laser interstitial thermal therapy (LITT) are too important for therapeutic purposes, especially for hyperthermia treatments. The purpose of this study was to determine a proper laser power and irradiation time for LITT applicator to irradiate liver tissue during hyperthermia treatment. For this aim, bioheat equation in one-dimensional spherical coordinate is solved by Green function method to simulate temperature distribution and rate of damage around irradiated target and how thermal and optical properties such as laser power, laser exposure time, and blood perfusion rate affect the rate of temperature distribution. Guiding equations according to the suggested boundary conditions are written and solved by MATLAB software. The outcomes show that increasing laser exposure time and power increase the temperature, especially at the nearest distance from the center of diffusion. Accordingly, a decrease in blood perfusion rate leads to decrease temperature distribution. The findings show that the model is useful to help the physicians to monitor the amount of heat diffusion by laser power during the treatment to protect healthy cells.**

***Index Terms*—Bioheat equation, Computational simulation, Green function, Hyperthermia, Laser interstitial thermal therapy.**

I. Introduction

Thermal therapies are considered minimally invasive techniques that are used to kill cancer cells with few or no harm to healthy tissue when part of the living body, for example, brain, prostate, or liver is exposed by external sources such as laser interstitial thermal therapy (LITT) (Chen, et al., 2021), radiofrequency (Wang, et al., 2015), or microwave ablation (Chu and Dupuy, 2014) to rise temperatures up to normal value. One of the approaches that can be used in non-invasive treatments is hyperthermia. It is a treatment mechanism among thermal therapies for treating normal and cancerous tissues by elevation the core temperature to nearly 50°C and below 40°C no measurable effects are observed (Niemz, 2019, Adeleh, et al., 2021). However, such treatments are done when conventional surgery either has less probability to success or too risky for the patient (Blauth, et al., 2020, Dutta and Kundu, 2018).

Among this clinical thermal procedure, the application of LITT is a promising technique that carries out under MRI or CT control to treat unresectable liver hepatic tumors and abnormalities. LITT is minimally invasive technique that performed by implanting a laser catheter in to the tumor cells due to hyperthermia and coagulative effects, Fig. 1. A specific beam of applied laser based on photon transport theory interacts with electric and magnetic properties of cell to increase the temperature at a sufficient level to destroy them (O'neal, Hirsch, and Halas, 2004, Andres, et al., 2020, Soares, et al., 2012). From the diffusion viewpoint, the transfer of thermal energy through living tissue depends on fundamental thermodynamic principles represented by bioheat transfer equations, which is very important to understand the process of temperature profiles (Ash, et al., 2017, Khaleel, Yahya, and Ibrahim, 2019).

As a matter of fact, therapy planning still is challenging problem and difficult issue because it is involving with many complicated thermal mechanisms that should be taken into account, such as metabolic heat generation, convection and blood perfusion rate, vascular structure, thermal conductivity, specific heat capacity of tissue, and biological conditions (Yassene and Verhey, 2005, Bhowmik, Singh, and Repaka, 2013) that are why there is not exit a unique model to give best accuracy. Moreover, the laser properties such as power and irradiation time are too significant which must be properly controlled to avoid unnecessary thermal damage of healthy cells and protect tissue from injuries by vaporization and carbonization. To handle these reasons, computational simulation can provide lots of potential benefits in clinical context to predict the degree of damage and temperature distribution around the catheter applicator that is absolutely necessary to understand the behavior

ARO-The Scientific Journal of Koya University
Vol. X, No. 2 (2022), Article ID: ARO.10949. 7 pages
DOI: 10.14500/aro.10949
Received: 04 March 2022; Accepted: 29 August 2022
Regular research paper: Published: 26 September 2022
Corresponding author's email: bazhdar.sh.mohammed@su.edu.krd

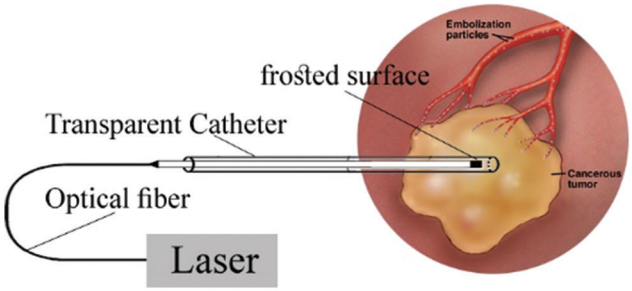

Fig. 1. Practical setup of laser interstitial thermal therapy for specific target. The optical fiber is sent to the liver tissue by means of specially designed (Niemz, 2019).

of increasing temperature in biological organs during the treatment to protect healthy cells.

Over the years, many governing mathematical equations have been proposed and modified since the middle of the last century when Penne's introduced his pioneering work about the distribution of temperature in the forearm (Pennes, 1948). A rate diffusion process model of laser-irradiated tissue has been proposed by Zhu, et al. (2002) to predict dynamic thermal response and the degree of injuries around the surface of applicator (Zhu, et al., 2002). In another work, the LITT model has been proposed to accurate modeling bioheat transfer mechanism and tissue response to thermal energy induced by different external thermal sources (Feng and Fuentes, 2011). Shibib, Munshid, and Lateef (2017) performed finite element method (FEM) to predict the physical properties of human liver tissue through the temperature distribution and measure the contagion damage volume by LITT (Shibib, Munshid, and Lateef, 2017). Andres, et al., have presented a numerical simulation to measure overestimated temperature until water vaporization in *ex vivo* porcine liver tissue. In Blauth, et al, 2020, a model simulated for LITT based on two approaches. In the first approach, radiation transport equation coupled with Pennes bioheat equation to estimate the temperature around coagulated region. In the second approach, LITT used for ablation purpose to transfer heat to *ex vivo* pig liver. A particular solution has been compared with nine test cases that have been measure using an optical fiber thermal diffuser applicator for delivering the rate of laser energy of neodymium-doped yttrium aluminum garnet (Nd: YaG) (Andres, et al., 2020). Furthermore, in Abbas, Hobiny, and Alzahrani, 2020, Giordano, Gutierrez, and Rinaldi, 2010, Li, Qin, and Tian, 2019, Özen, Helhel, and Cerezci, 2008, Skandalakis, et al., 2020, Vogl, et al., 2004, Zhou, Chen, and Zhang, 2007, various techniques have been used to predict the temperature distribution in biological tissue during the treatments.

In this study, a new method is approached to predict the effect of thermal and optical properties of LITT during liver treatment by hyperthermia. The parameters are conducted to Pennes bioheat equation and solved in one-dimensional spherical coordinate based on Green function to predict how liver tissue affected by laser power, exposure time, and blood perfusion rate as well as estimate the degree of damage produced by radiative LITT technique. For this purpose, a Nd: YaG laser at a wavelength 1064 nm is used because of high penetration depth. In addition, the results compared with an existence computational model. The findings show that the current computational model is effective tool for predicting the degree of liver tissue damage through LITT power and helpful to control the amount of heat diffusion during the treatment.

II. Mathematical Formulation and Solution of the Problem

For the modeling, surface diffusion type of LITT applicator is considered to transfer thermal energy to the tissue (Niemz, 2019). Furthermore, to keep the variance of the temperature profiles by LITT, vascular structures of liver tissue are considered to be uniformly distributed and spherically diffused. The model summarizing in to two boundary parts: The first part located at the center of diffusing that corresponds to the interface between the laser applicator and tissue and the second part refers to ambient body temperature, Fig. 1. The transient problem is demonstrated based on bioheat equation which is given by Zhu, et al., 2002. For simplicity, it is being assuming tissue has constant thermal properties and the medium of heat diffusion is non-isotropic:

$$\rho c\frac{\partial T(r,t)}{\partial t}=\nabla.\left(k\nabla \mathrm{T(r,t)}\right)+\rho_b c_b \omega_b (T_c-T(r,t))+Q_m+Q_{ext}\ , \tag{1}$$

Where, t is t time and T is the temperature distribution, ρ and c are tissue density and specific heat capacity, respectively. k is tissue thermal conductivity, T_c is tissue surface temperature at the boundary of sphere. ρ_b is density of blood, c_b is blood-specific heat capacity, ω_b is blood perfusion rate term represents the effect of blood flow in vessels or microcapillaries, Q_m is a metabolic rate due to the basal metabolism, and Q_{ext} represents external heat generation.

To solve this, inhomogeneous partial differential operator a Green function is performed which belongs to the instantaneous point source (Faryad and Lakhtakia, 2018). Green's function operator is defined corresponding to the boundary conditions of the system to the action of laser beam pulse as an external heat source acting at an any distance (r) from the center of diffusion and at any time (t) (Hahn and Özisik, 2012). Now, Equation (1) can be rearranged and rewritten by introducing a new variable $\Theta = T\text{-}T_c$ and the linear differential operator L to give more suitable mathematical form (Hobiny et al., 2021):

$$\left(\frac{\partial}{\partial t}+\beta\nabla^2+\alpha^2\right)\theta_{(r,t)}=L_1\left(\theta_{(r,t)}\right)=\frac{Q}{\rho c}\ , \tag{2}$$

Where, $\alpha^2=\frac{\omega_b c_b \rho_b}{\rho c}$, $\beta=\frac{k}{\rho c}$, and $Q=Q_m+Q_{ext}$. To find basic solution for this differential operator, we start from Green's characteristic equation:

$$L_1\left(G_{(r,t|r',\tau)}\right)=\delta\left(r,r'\right)\delta\left(t,\tau\right)\ , \tag{3}$$

 http://dx.doi.org/10.14500/aro.10949

Where, G is Green's function and δ is the Dirac delta function. If the domain unbounded the general representation of Green's function, the equation denoted by $V\left(r,t|r',\tau\right)$. In this case, Equation (2) in a radial coordinate can be written as:

$$L_1\left(V\right)=\left(\frac{\partial}{\partial t}+\beta\frac{\partial^2}{\partial r^2}-\frac{2\beta}{r}\frac{\partial}{\partial r}+\alpha^2\right)V=\frac{\delta(r-r')\delta(t-\tau)}{4\pi r^2} \tag{4}$$

The solution of this problem can be determined by the method of separation of variables and applying the inverse Fourier transform (the detail about solving steps can be found in Feng and Fuentes, 2011). Once the equation is solved, the principal solution part is:

$$V_{\left(r,t|r',\tau\right)}=\frac{2H_{(t-\tau)}e^{-\alpha^2(t-\tau)}}{\pi rr'}\int_{\lambda=0}^{\infty}e^{-\lambda\alpha^2(t-\tau)}\sin\left(\lambda r\right)\sin\left(\lambda r'\right)d\lambda\,, \tag{5}$$

$H_{(t-\tau)}$ is the Heaviside step function. Equation (5) is a closed form of the analytical solution. Now, the final radial solution can be expressed as the following:

$$V_{\left(r,t|r',\tau\right)}=\frac{H_{(t-\tau)}e^{-a^2(t-\tau)}}{2\pi r'\sqrt{\beta\pi(t-\tau)}}\left[e^{\frac{-(r-r')^2}{4\beta(t-\tau)}}-e^{\frac{-(r+r')^2}{4\beta(t-\tau)}}\right] \tag{6}$$

.

Now, the Green's function solution equation (GFSE) should be introduced, which is a general expression that provides a non-linear temperature distribution in a medium based on suitable boundary conditions. Here, for the particular case of Equation 4, the GFSE for spherical coordinate is given by Hahn and Özisik, 2012:

$$\theta\left(r,t\right)=\int r'^{p}V_{\left(r,t|r',\tau\right)\tau=0}F\left(r'\right)dr'+\frac{\beta}{k}\int_{\tau=0}^{t}\int r'^{p}V_{\left(r,t|r',\tau\right)}Q\left(r,\tau\right)dr\,d\tau \tag{7}$$

,

Where, $V_{\left(r,t|r',\tau\right)}$ is closed form solution at $\tau=0$, $F\left(r'\right)$ represents initial conditions. r'^{p} is the Sturm–Liouville weighting function.

A. Boundary conditions

For the boundary conditions, it is supposed that the core and the surrounding temperature of spherical tissue are constant before applying external source. By the same fact, the boundary temperature at any region far from the core of the sphere is also constant.

$$T\left(r,0\right)=T_c\,,\ \left(\partial T(r,0)\right)/\partial t=0\,, \tag{8}$$

$$\left[T\left(r,t\right)\right]_{r\to\infty}=T_s\,,\ \left(\left[\partial T(r,0)\right]\_(r\to\infty)\right)/\partial t=0 \tag{9}$$

B. Laser heat source

As infrared laser beam (Nd: YaG) interacts with the region of interest, the diffusion of heat around the area of interaction mainly depends on the absorption coefficient μ_a (Milanic, et al., 2019, Ash, et al., 2017):

$$Q_{ext}(r)=\frac{\mu_a\left(1-R_l\right)Pe^{-(\mu_a+(1-g)\mu_s)r}}{4\pi r^2}\,, \tag{10}$$

Where, R_l is the light reflectivity of tissue depends on laser wavelength, P is a laser power releasing, it is energy at close g point to the center $r=r_0$ and spontaneously at t=0. μ_s is scattering coefficient, g is anisotropy factor its range between −1 and 1, in case of forward scattering g = 1, isotropic scattering g = 0, and g = −1 for backward scattering.

C. Mathematical formulation

The temperature distribution in one-dimensional spherical coordinate can be represented as the following:

$$\frac{\partial\theta_{(r,t)}}{\partial t}=\frac{\beta}{r^2}\frac{\partial}{\partial r}\left(r^2\frac{\partial\theta_{(r,t)}}{\partial r}\right)-\alpha^2\theta_{(r,t)}+\frac{Q}{\rho c}\,,\quad (t>0\,;0<r<\infty) \tag{11}$$

then, boundary conditions have been given in Equations (8) and (9)

$$\theta\left(r,0\right)=T_c\,,\ \left(\partial\theta(r,0)\right)/\partial t=0\,. \tag{12}$$

$$\left[\theta\left(r,t\right)\right]_{r\to\infty}=T_c\,,\ \left(\left[\partial\theta(r,0)\right]\_(r\to\infty)\right)/\partial t=0\,. \tag{13}$$

the homogenous solution in terms of Green's function is expressed as:

$$\theta1\left(r,t\right)=\int r'^{p}V_{\left(r,t|r',\tau\right)\tau=0}F\left(r'\right)dr'\,. \tag{14}$$

and the inhomogeneous solution of Equation (7) in terms of Green's function is found to be:

$$\theta2\left(r,t\right)=\frac{\beta}{k}\int_{\tau=0}^{t}\int r'^{p}V_{\left(r,t|r',\tau\right)}Q\left(r\right)dr\,d\tau\,. \tag{15}$$

the overall temperature distribution solution is obtained by adding homogenous and inhomogeneous solutions:

$$\theta\left(r,t\right)=\int r'^{p}V_{\left(r,t|r',\tau\right)\tau=0}F\left(r'\right)dr'+\frac{\beta}{k}\int_{\tau=0}^{t}\int r'^{p}V_{\left(r,t|r',\tau\right)}Q\left(r\right)dr\,d\tau\quad . \tag{16}$$

by putting the boundary conditions, putting P = 2 for the spherical coordinate system (Beck, et al, 1992), $F\left(r'\right)=0$, and laser heat source equation. The Equation (16) reduced to:

$$\theta\left(r,t\right)=\frac{\beta}{k}\int_{\tau=0}^{t}\int_{r'=0}^{\infty}r'^{2}V_{\left(r,t|r',\tau\right)}\left(Qm+\frac{\mu_a\left(1-R_l\right)Pe^{-\mu_a r}}{4\pi r^2}\right)dr'd\tau\,, \tag{17}$$

The integral $\int_{r'=0}^{\infty}r'^{2}V_{\left(r,t|r',\tau\right)}\left(\frac{\mu_a\left(1-R_l\right)Pe^{-\mu_a r}}{4\pi r^2}\right)dr'$ can be solved numerically according to the given laser source equation along with $V_{\left(r,t|r',\tau\right)}$ into the equation, the expression becomes:

$$\frac{\beta}{k}\int_{\tau=0}^{t}\int_{r'=0}^{\infty} r'^{2} V_{(r,t|r',\tau)}\left(\frac{\mu_a(1-R_l)Pe^{-\mu_a r}}{4\pi r^2}\right)dr'd\tau$$

$$=\frac{\mu_a(1-R_l)P}{8\pi krr_0}\int_{\tau=0}^{t}\frac{e^{-(\alpha^2(t-\tau)+\mu_a r')}}{\sqrt{\beta\pi(t-\tau)}}\left[e^{\frac{-(r-r')^2}{4\beta(t-\tau)}}-e^{\frac{-(r+r')^2}{4\beta(t-\tau)}}\right]\ d\tau \quad , \tag{18}$$

On the other hand, the radial integral of $\int_{\tau=0}^{t}\int_{r'=0}^{\infty} r'^{2} V_{(r,t|r',\tau)} Qm\, dr'd\tau$ represents Dirac delta function integral over the entire line which is equal to one (Modest, and Mazumder, 2021) and the time integral can be determined analytically. Finally, the solution reduces to:

$$\frac{\beta}{k}\int_{\tau=0}^{t}\int_{r'=0}^{\infty} r'^{2} V_{(r,t|r',\tau)} Qm\, dr'd\tau = \frac{\beta Qm}{k\alpha^2}(1-e^{-(\alpha^2 t)}). \tag{19}$$

by putting the results of last two equations into Equation (17), the final solution of temperature distribution is $T(r,t)=Tc+\theta(r,t)$ which can be expressed as:

$$T(r,t)=Tc+\frac{\beta Qm}{k\alpha^2}\left(1-e^{-(\alpha^2 t)}\right)+\frac{\mu_a(1-R_l)P}{8\pi krr_0}$$
$$\int_{\tau=0}^{t}\frac{e^{-(\alpha^2(t-\tau)+\mu_a r')}}{\sqrt{\beta\pi(t-\tau)}}\left[e^{\frac{-(r-r')^2}{4\beta(t-\tau)}}-e^{\frac{-(r+r')^2}{4\beta(t-\tau)}}\right]d\tau \tag{20}$$

III. Results and Discussion

In this section, the variation of temperature in liver tissue is estimated according to different LITT laser powers, duration times, and blood perfusion rates. To obtain the results, a computer program by MATLAB R2016a language is written. All the figures are drawn which are obtained from final solution of Equation 20, then integration over time is applied numerically by Simpson approximation rule after sorting temperature for each r at a fixed t. In addition, we considered $r_0 = 0.00075m$ to get the solution from the final equation. Regarding to a Nd: YaG laser properties, the value of R_l is 5%. The values of blood perfusion rate have been repossessed from Niemz, 2019, Adeleh, et al., 2021.It usually changes between 0.001 s^{-1} and 0.0005 s^{-1}. Furthermore, the diffusion domain is considered a sphere of radius (R) of 2 cm. Exemplary values of thermodynamic and optical properties have been retrieved from reference (Blauth, et al., 2020) and supposed to be constant throughout the domain, Table I.

Table I
Physical and Optical Parameters for Laser Interstitial Thermal Therapy in Liver Tissue

Parameter	Value
μ_a	50 m^{-1}
μ_s	8000 m^{-1}
G	0.97
ρ_b	1137 kg/m^3
C_b	3640 (J.kg)/k
K	0.518 W/(m.k)
P	1000 kg/m^3
C	4187 (J.kg)/k

A. The effect of irradiation time

Fig. 2 shows the effect of the different laser irradiation time (τ =5.10 and 15 s) on the temperature profiles along the radial distance (r) when the laser power and blood diffusion rate are constants. Whenever the laser source is switched off, the maximum temperature is recorded at the center of the desired zone and then it decreases exponentially to the normal temperature T=36.8°C. Due to the long wavelength of used laser, which is located near-infrared region in the electromagnetic spectrum, an increase in time causes rise in temperature. It is clear that the longer exposure time produced a peak temperature just below 50°C which is the maximum limit of temperature to make hyperthermia whereas it is beyond that this value might cause reduction in enzyme activity resulting decrease to energy transfer between the cell and its surroundings, cell membrane disorder, and coagulation phenomena. As we can see even at maximum exposure time, the surrounding healthy cells are preserved.

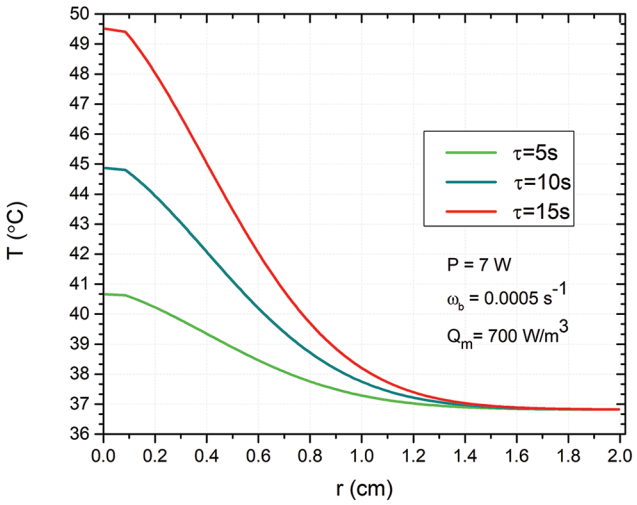

Fig. 2. Transient temperature distribution as a function of radius in liver tissue for different values of laser irradiation time (laser on).

The resulting of temperature change at 10 s laser intensity 120 Kw/m^2 is found to be very close to that achieved by Abbas, Hobiny, and Alzahrani, 2020. As can be noticed from Fig. 3, there is no much difference between temperatures in smaller radius whereas at 0.8–2 cm, the average change in temperature between this work and reference (Abbas, Hobiny, and Alzahrani, 2020) is only 1°C.

Alternately, at a given radius, the relation between the laser exposure time and temperature distribution is linear (Fig. 4). On the other side, when exposure time remains constant at 25 s, the variation of temperature between r = 0.3 cm and r

http://dx.doi.org/10.14500/aro.10949

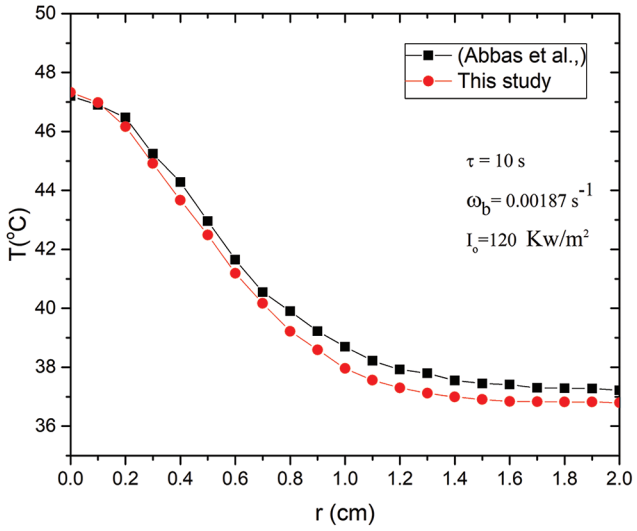

Fig. 3. Comparison between the centerline temperature obtained by this model and reference (Abbas, Hobiny, and Alzahrani, 2020) at constant laser intensity and exposure time.

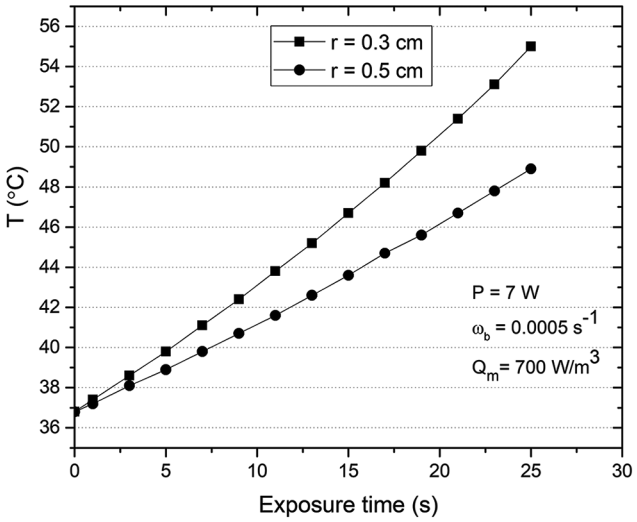

Fig. 4. Relation between temperature achieved and exposure time for two different distances.

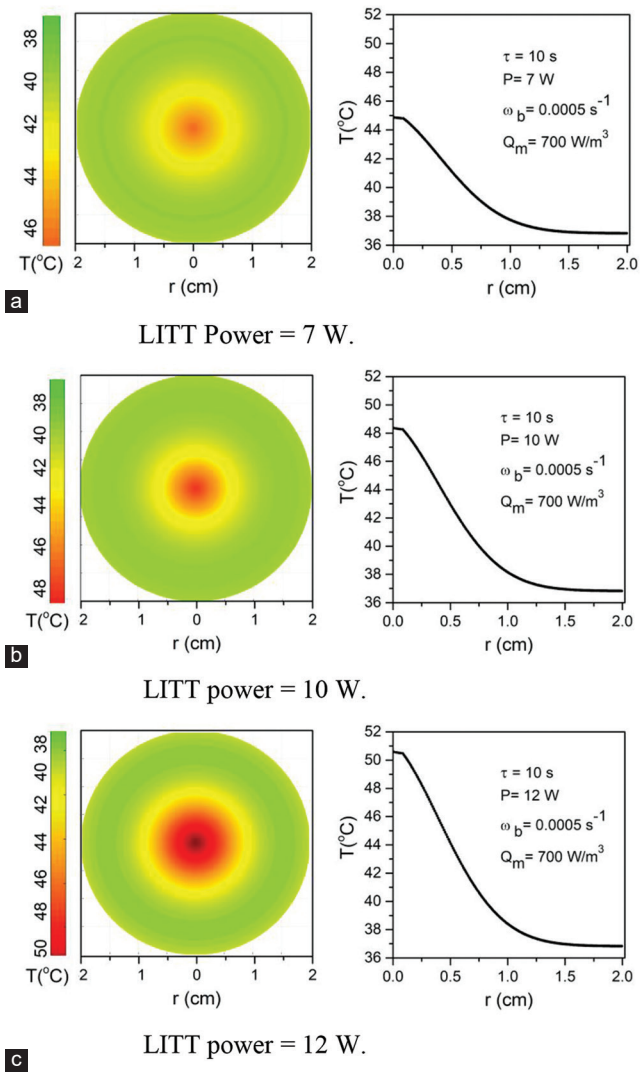

Fig. 5. Two-dimensional temperature contours and temperature profile as a function of distance for different laser powers. (a) and (b) achieved temperature change by laser interstitial thermal therapy with P = 7 and 10 W do not exceed hyperthermia conditions and (c) P=12 W more heat is generated and absorbed in the tissue which beyond hyperthermia condition.

= 0.5 cm is about 6°C as well as temperature still remains in hyperthermia range for smaller radius; meanwhile, it reaches the coagulation disorders in greater radius that necrotizing the healthy cells.

B. The effect of laser power

Fig. 5 illustrates the graphical representation of the temperature variation from the center of the desired target to sphere boarder. The tissue is irradiated by three different laser powers with beam radius 0.5 mm in constant exposure time and blood perfusion rate during the cooling process (laser off). It is to be noted as a power of laser irradiation increased, more energy is absorbed by the tissue which is subsequently transform into thermal energy, especially at the nearest surroundings. In contrast, low concentration laser power causes a weak thermal response. In Fig. 5a and b as can be observed, under the given conditions, almost all healthy cells are not damaged and could be recovered after treatment whereas in Fig. 5c, the central part temperature profile higher than hyperthermia limit resulting repair mechanism of the cell is disabled. At a radial distance 2 cm from the irradiated point, the temperature is close to normal liver temperature for the suggested laser powers.

C. The effect of blood perfusion rate

Fig. 6 represents the effect of different blood perfusion rate on temperature distribution in a given laser power exposure time during the cooling process to investigate the hyperthermia phenomena.

It is shown that reducing blood perfusion rate from 0.0005 s^{-1} to 0 s^{-1} that causes temperature increased by approximately 5°C because decreasing blood perfusion rate means less energy

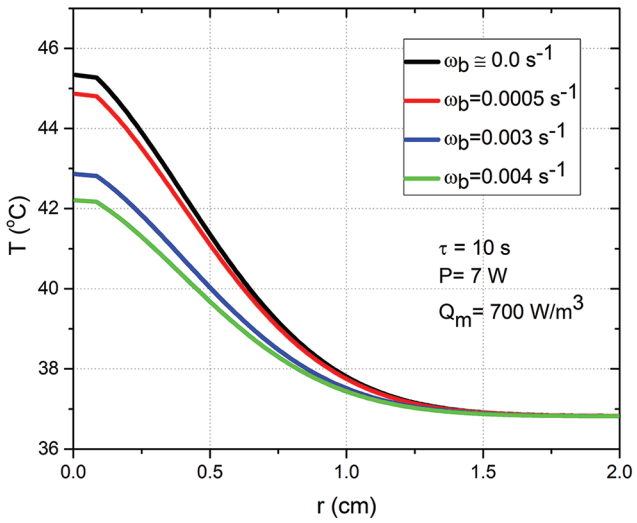

Fig. 6. Impact of blood perfusion rate on heat diffusion in a given time and power.

exchange between the blood capillaries and tissue surroundings due to implement less heat with low blood flow. Overall, the figure shows that under the given constant parameters change blood perfusion rate do not affect the healthy cells because the temperatures located in the range needed for hyperthermia.

IV. Conclusion

Bioheat transfer simulation is extensively useful in thermotherapy applications such as hyperthermia for accurately evaluating heat diffusion in tissue during the treatment. LITT is a minimally invasive therapeutic technique approved for heating a liver tissue and other anatomical regions. Still there does not exist a unique model to describe heat transfer in biological tissue by LITT because the process is involved with many complex phenomena. In this study, a Green function method is used to solve bioheat equation according to thermal and optical properties of LITT to predict amount of heat transfer to liver tissue during hyperthermia treatment. The model shows how the laser power and exposure time are controlled to protect the healthy cells around the damaged zone. The results from this study are compared with the results of other published data (Abbas, Hobiny, and Alzahrani, 2020). It can be observed increase LITT power and exposure time causes increase thermal damage volume. Furthermore, heat diffusion and rate of damage are inversely proportional with blood perfusion rate. The suggested Nd-YaG laser power for liver hyperthermia treatment is 7–10 W with exposure time of 10 s. This approach can be useful before beginning the treatment to correctly predict the diffused temperature and monitor it during the treatment. However, this model is simulated for hyperthermia treatment only, under semi-homogenous system and symmetrical geometry. In further study, more accurate conditions could be added to develop the model to shrink tumors by damaging tissue through thermal coagulation and get better estimation about heat diffusion.

References

Abbas, I., Hobiny, A. and Alzahrani, F. 2020. An analytical solution of the bioheat model in a spherical tissue due to laser irradiation. *Indian Journal of Physics*, 94(9), pp.1329-1334.

Adeleh, K., Reza, H., Mohammed, M. and Hossein, A. 2021. Numerical study on the effect of blood perfusion and tumor metabolism on tumor temperature for targeted hyperthermia considereing a realistic geometrical model of head layers using the finite element method. *SN Applied Sciences*, 3(4), pp.1-17.

Andres, M., Blauth, S., Leithäuser, C. and Siedow, N. 2020. Identification of the blood perfusion rate for laser-induced thermotherapy in the liver. *Journal of Mathematics in Industry*, 10(1), p.17.

Ash, C., Dubec, M., Donne, K. and Bashford, T. 2017. Effect of wavelength and beam width on penetration in light-tissue interaction using computational methods. *Lasers in Medical Science*, 32(8), pp.1909-1918.

Beck, J.V., Cole, K.D., Haji-Sheikh, A. and Litkouhl, B. 1992. *Heat Conduction Using Green Function*. Taylor and Francis., New York. p.552.

Bhowmik, A., Singh, R. and Repaka, R. 2013. Conventional and newly developed bioheat transport models in vascularized tissues: A review. *Journal of Thermal Biology*, 38(3), pp.107-125.

Blauth, S., Hübner, F., Leithäuser, C., Siedow, N. and Vogl, T.J. 2020. Mathematical modeling of vaporization during laser-induced thermotherapy in liver tissue. *Journal of Mathematics in Industry*, 10(1), pp. 1-16.

Chen, C., Lee, I., Tatsui, C., Elder, T. and Sloan, A.E. 2021. Laser interstitial thermotherapy (Litt) for the treatment of tumors of the brain and spine: A brief review. *Journal of Neuro Oncology*, 151(3), pp.429-442.

Chu, K. and Dupuy, D. 2014. Thermal ablation of tumours: Biological mechanisms and advances in therapy. *Nature Reviews Cancer*, 14(3), pp.199-208.

Dutta, J. and Kundu, B. 2018. Thermal wave propagation in blood perfused tissues under hyperthermia treatment for unique oscillatory heat flux at skin surface and appropriate initial condition. *Heat and Mass Transfer*, 54(11), pp.3199-3217.

Faryad, M. and Lakhtakia, A. 2018. *Infinite-Space Dyadic Green Functions in Electromagnetism*. Morgan and Claypool Publishers, San Rafael, California.

Feng, Y. and Fuentes, D. 2011. Model-based planning and real-time predictive control for laser-induced thermal therapy. *International Journal of Hyperthermia*, 27(8), pp.751-761.

Giordano, M., Gutierrez, G. and Rinaldi, C. 2010. Fundamental solutions to the bioheat equation and their application to magnetic fluid hyperthermia. *International Journal of Hyperthermia*, 26(5), pp.475-484.

Hahn, D. and Özisik, M. 2012. *Heat Conduction*, John Wiley and Sons, United States.

Soares, P.I.P., Ferreira, I.M.M., Igreja, R.A.G., Novo, C.M.M. and Borges, J.P.M. 2012. Application of hyperthermia for cancer treatment: Recent patents review. *Recent patents on anti-cancer drug discovery*, 7(1), pp.64-73.

Khaleel, Y., Yahya, S. and Ibrahim, R. 2019. Skin temperature distribution over human head due to handheld mobile phone call using thermal imaging camera. *Aro-The Scientific Journal of Koya University*, 7(2), pp.63-68.

Li, X., Qin, Q.H. and Tian, X. 2019. Thermomechanical response of porous biological tissue based on local thermal non-equilibrium. *Journal of Thermal Stresses*, 42(12), pp.1481-1498.

Milanic, M., Muc, B.T., Lukac, N. and Lukac, M. 2019. Numerical study of hyper-thermic laser lipolysis with 1,064 nm Nd: Yag laser in human subjects. *Lasers in Surgery and Medicine*, 51(10), pp.897-909.

Modest, F. and Mazumder, S. 2021. *Radiative Heat Transfer*, Academic Press, United States.

Niemz, M., 2019. *Laser-Tissue Interactions*, Springer, Germany.

O'neal, D., Hirsch, L. and Halas, N. 2004. Photo-thermal tumor ablation in mice

using near infrared-absorbing nanoparticles. *Cancer Letters*, 209(2), pp.171-176.

Özen, S., Helhel, S. and Cerezci, O. 2008. Heat analysis of biological tissue exposed to microwave by using thermal wave model of bio-heat transfer (TWMBT). *Burns*, 34(1), pp.45-49.

Pennes, H. 1948. Analysis of tissue and arterial blood temperatures in the resting human forearm. *Journal of Applied Physiology*, 1(2), pp.93-122.

Shibib, K., Munshid, A. and Lateef, H. 2017. The effect of laser power, blood perfusion, thermal and optical properties of human liver tissue on thermal damage in LITT. *Lasers in Medical Science*, 32(9), pp.2039-2046.

Skandalakis, G., Rivera, D., Rizea, C., Bouras, A., JesuRaj, J., Bozec, D. and Hadjipanayis, C. 2020. Hyperthermia treatment advances for brain tumors. *International Journal of Hyperthermia*, 37(2), pp.3-19.

Vogl, T., Straub, R., Zangos, S., Mack, M. and Eichler, K. 2004. Mr-guided laser-induced thermotherapy (LITT) of liver tumours: Experimental and clinical data. *International Journal of Hyperthermia*, 20(7), pp.713-724.

Wang, K., Tavakkoli, F., Wang, S. and Vafai, K. 2015. Analysis and analytical characterization of bioheat transfer during radiofrequency ablation. *Journal of Biomechanics*, 48(6), pp.930-940.

Mohammed, Y. and Verhey, J.F. 2005. A finite element method to simulate laser interstitial thermotherapy in anatomical inhomogenous regions. *Biomedical Engineering Online*, 4(1), p.2.

Zhou, J., Chen, J. and Zhang, Y. 2007. Theoretical analysis of thermal damage in biological tissues caused by laser irradiation. *Molecular and Cellular Biomechanics*, 4(1), pp.27.

Zhu, D., Luo, Q., Zhu, G. and Liu, W. 2002. Kinetic thermal response and damage in laser coagulation of tissue. *Lasers In Surgery And Medicine: The Official Journal of The American Society For Laser Medicine and Surgery*, 31(5), pp.313-321.